Characterization of Solvent-Spun Polyester Nanofibers

S. Duzyer,[1] A. Hockenberger,[1] E. Zussman[2]

[1]*Department of Textile Engineering, Uludag University, Bursa 16059, Turkey*
[2]*Faculty of Mechanical Engineering, Technion–Israel Institute of Technology, Haifa 32000, Israel*

Received 19 October 2009; accepted 9 July 2010
DOI 10.1002/app.33092
Published online 3 November 2010 in Wiley Online Library (wileyonlinelibrary.com).

ABSTRACT: The aim of this study was to examine the properties of polyester nanofibers produced by the electrospinning method. Solvent-spun nanofibers with different concentrations of poly(ethylene terephthalate) (13, 16, and 20 wt %) were produced. The morphology and surface energy of the fibers were analyzed by scanning electron microscopy and contact angle measurements. Tensile testing, dynamic mechanical analysis, and differential scanning calorimetry were carried out to characterize the thermal and mechanical properties. X-ray diffraction and attenuated total reflection Fourier transform infrared spectroscopy tests were performed to analyze the microstructural properties. The results show that a nanoweb of the 16 wt % solution had better mechanical and thermal behaviors because of the increased molecular orientation in the amorphous structure and the narrower fiber diameter distribution in the web. © 2010 Wiley Periodicals, Inc. J Appl Polym Sci 120: 759–769, 2011

Key words: fibers; mechanical properties; nanotechnology; polyesters; surfaces

INTRODUCTION

Synthetic fibers are increasingly being used both in high-technology textiles and home textiles because of their unique properties and relatively low cost. Extensive research has been carried out to characterize these materials and their applications. Structural and surface modifications of well-known synthetic fibers have received a great deal of attention from both textile engineers and polymer and material scientists as the cost of research to develop new materials is high and requires a great deal of time. The fineness of the textile fiber is very important in terms of many properties; such as the surface area, adhesion, and mechanical performance. A reduction in the fiber diameter increases the specific surface area and enhances the mechanical performance. When diameter reaches nanodimensions, the surface characteristics, then, become very important for the performance.

Nanofibers are produced by melt-blowing, spunbonding, fibrillation, bicomponent fibers, and electrospinning. Electrospinning is a simple technique for the production of nanofibers. Electrospinning is a straightforward method for producing nanofibers from polymer solutions or polymer melts in a wide submicrometer range around 100 nm.[1]

Correspondence to: A. Hockenberger (sengonul@uludag.edu.tr).

Journal of Applied Polymer Science, Vol. 120, 759–769 (2011)

The electrospinning process involves the application of a strong electrostatic field to a capillary connected to a reservoir containing a polymer solution. Under the influence of the electrostatic field, a pendant droplet of the polymer solution at the capillary tip is deformed into a conical shape (Taylor cone). If the voltage surpasses a threshold value, electrostatic forces overcome the surface tension, and a fine charged jet is ejected. The jet moves toward a ground plate acting as a counter electrode. Because of the viscosity of the polymer solution and the presence of entanglements, the jet remains stable and does not transform into spherical droplets as expected for a liquid cylindrical thread. The solvent begins to evaporate immediately after the jet is formed. The result is the deposition of a thin polymer fiber on a substrate located above the counter electrode.[2–4]

The description of the process suggests that the following parameters affect the process: the solution properties, including viscosity, conductivity, and surface tension; controlled variables, including hydrostatic pressure in the capillary, electric potential of the tip, and the distance between the tip and the collection screen; and ambient parameters, including temperature, humidity, and air velocity in the electrospinning chamber. The electrospinning of the polymer solution or melts can produce nanofiber webs.[5] Nanofibers can have different mechanical properties than those with larger diameters.[6,7] As the fiber diameter decreases, the surface plays a more important role in the determination of the properties than those of the bulk material. Considerable attempts have been made in the last few years

to describe the electrospinning process and the parameters that affect fiber formation.[8–12]

Poly(ethylene terephthalate) (PET) is a linear polymer and is widely used in textiles. It has a unique combination of physical and chemical properties. Several researchers have studied the properties and applications of electrospun PET nanofibers. Kim et al.[13] evaluated the effect of the molecular weight of the polymer on electrospun PET nonwovens and their mechanical properties as a function of the linear velocity of the drum surface. They reported that the mechanical properties of the electrospun PET nonwovens were strongly dependent on the linear velocity of the drum surface. They also found that the polymer took on a particular molecular orientation when the linear velocity of the drum surface was increased to 45 m/min. The characteristics of the electrospinning technique, such as the high porosity, small pore sizes with an interconnected structure, and a large surface area per unit volume, make it attractive in a variety of applications, including both air and fluid filtration. A PET nanofibrous electrospun membrane was used as a filtration membrane for juice clarification.[14] PET was selected as the polymer to prepare nanofibrous mats because of its low cost, attractive structural and mechanical characteristics, and good electrospinning properties. The hydraulic permeabilities of PET electrospun fiber webs were also investigated[15] and compared with spunbond nonwoven fabrics. The water vapor transport rates of PET electrospun fiber webs were higher than those of PET spunbonds. The polymer blends of PET and chitosan were electrospun onto the PET micro-nonwoven mats for biomedical applications. Researchers reported that the PET/chitosan nanofiber mats showed a significantly higher growth inhibition rate compared with the PET nanofiber control and that the fibroblast cells adhered better to the PET/chitosan nanofibers than to the PET nanofibers mats; this suggested better tissue compatibility.[16]

Nonwoven PET nanofiber mats were prepared by electrospinning technology and were surface-modified to mimic fibrous proteins in the native extracellular matrix for the construction of a biocompatible surface for endothelial cells.[17] Lopes-da-Silva et al.[18] reported the preparation and characterization of nanofibrous mats electrospun from mixed solutions of PET and chitosan, with potential applications in such areas as filtration, tissue scaffolds, and protective clothing.

Most of the research on PET nanofibers been done on the different application areas and performance tests according to these application areas. The aim of this study was to examine the thermal and mechanical properties of polyester nanofibers produced by the electrospinning method. Scanning electron microscopy (SEM) and contact angle (θ) measurements were carried out to identify the morphology and surface characteristics of the nanofibers. Tensile tests, dynamic mechanical analysis (DMA), and differential scanning calorimetry (DSC) were performed to determine the mechanical and thermal properties of the nanofibers, and X-ray tests and attenuated total reflection (ATR) Fourier transform infrared (FTIR) spectroscopy were performed to analyze the internal structure of the nanofibers.

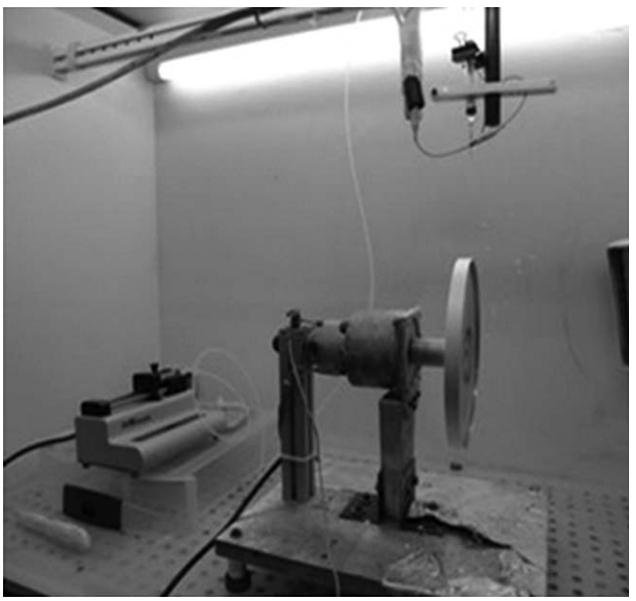

Figure 1 Experimental electrospinning setup.

EXPERIMENTAL

Materials

PET chips were commercially available and were used in this study to produce the nanofibers. The viscosity of the chips was 0.645 P. The chemicals dichloromethane (DCM) and trifluoroacetic acid (TFA) were used as solvents to dissolve the PET polymer. All chemicals were used as received without any further purification. All chemicals were commercially available from Sigma-Aldrich (Haifa, Israel). Solutions of PET at different concentrations were prepared by the dissolution of PET chips in TFA (50 wt %) and DCM (50 wt %) solvent mixture.

A rotating disk was used to collect samples for SEM and tensile tests. A sharp disk was used to collect samples for X-ray analysis.

Electrospinning process

Figure 1 shows the image of the experimental apparatus. The electrospinning apparatus used in this study consisted of a syringe attached to a capillary tip, a syringe pump, a collector, and a high-voltage supply. The jet flowed downward from the surface of a pendant drop of fluid toward a rotating disc collector at a

distance of 100 mm below the droplet. An electric potential difference of 9 kV was created between the surface of the liquid drop and the rotating disc collector. The linear speed of the edge of the disk collector was 2.7 m/s. The polymer solution was electrospun from a plastic syringe with an internal diameter of about 25 G (=0.455 mm) and with a flow rate of 1 mL/h. At the beginning of the experiment, a pendant droplet of polymer solution was supported at the tip of the syringe. When the potential difference between the droplet and the grounded wheel was increased, the droplet acquired a conelike shape (Taylor cone). At a certain potential difference, a stable jet emerged from the cone and moved downward toward the collector. All experiments were carried out in air at room conditions. After electrospinning, no further processing was applied to the fibrous webs.

SEM analysis

The morphology of the electrospun fibers was examined by SEM. The specimens for high-resolution SEM were prepared by direct deposition of the electrospun nanofibers onto a piece of silicon wafer. The morphology of the electrospun fibers was observed with SEM after gold coating. The micrographs were obtained by a secondary scattered electrons detector with a Leo Gemini 982 high-resolution scanning electron microscope (Technion-Israel Institute of Technology, Haifa, Israel).

Viscosity measurements

The viscosity of the solutions with different PET concentrations (13, 16, and 20 wt %) were measured by a Mesdan Lab Hooke Viscotester 7 Plus at 60 rpm (Istanbul Textile & Apparel Research & Development Center, Istanbul, Turkey). The temperature of the solutions was approximately 19°C.

ATR–FTIR spectrometry

A PerkinElmer Spectrum 400 FTIR spectrometer (The Science and Technology Park of Kayseri, Kayseri, Turkey) was used for IR measurements with a single-reflection diamond-based GladiATR model ATR attachment (The Science and Technology Park of Kayseri). IR dichroic measurements were carried out with a KRS-5 based polarizer (The Science and Technology Park of Kayseri, Kayseri, Turkey) located before the sample. All of the spectra were collected in the mid-IR range (i.e., 4000–400 cm^{-1}) at a resolution of 2 cm^{-1}. Finally, all of the spectra were analyzed with OMNIC software to obtain accurate peak parameters (The Science and Technology Park of Kayseri, Kayseri, Turkey). Figure 2 shows the polarized IR sampling geometries showing the relative position of polarizer and the sample.[19]

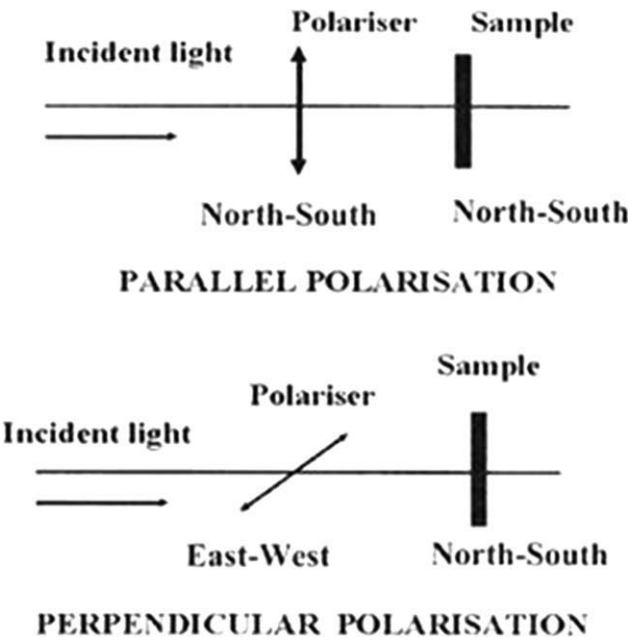

Figure 2 Polarized IR sampling geometries showing the relative positions of the polarizer and the sample.

X-ray analysis

X-ray diffraction analysis of the PET electrospun nanofiber web was performed on a Bruker AXS Nanostar diffractometer (The Science and Technology Park of Kayseri, Kayseri, Turkey). The X-ray beam was directed parallel to the normal of the fiber bundle so the beam was perpendicular to the winding direction of the nanofibers. The scans were recorded at room temperature with 2θ's ranging from 5 to 35°.

Wide-angle X-ray scattering was performed with a small-angle diffractometer (Bruker AXS Nanostar, tube: KFF CU 2 K-90) with Cu Kα radiation at a wavelength of 0.15418 nm with pinhole collimation (that resulted in a beam 100 μm in diameter), and a 10 × 10 cm^2 two-dimensional position-sensitive wire detector was positioned 7.63 cm behind the examined sample.

DSC analysis

DSC analysis was performed on a Sapphire model test machine by PerkinElmer. The 13, 16, and 20 wt % solution samples were 1.2, 1.55, and 3.02 mg, respectively. The samples were ramped from room temperature to 300°C. The scanning rate was 10°C/min.

Tensile tests

The tensile tests were carried out on DMA Q800 test machine (Technion-Israel Institute of Technology, Haifa, Israel). The tests were performed on webs of aligned fibers. Rectangular specimens containing 13, 16, and 20 wt % solutions with dimensions of 12 × 5 × 0.085, 12 × 5 × 0.083, and 12 × 5 × 0.140 mm, respectively, were mounted on tension clamps. The

PET nanofiber webs were subjected to stress–strain testing with a strain rate of 1%/min.

DMA tests

A DMA Q800 test machine was used to study the dynamic mechanical behavior of the specimens (Technion-Israel Institute of Technology, Haifa, Israel). Rectangular specimens containing 13, 16, and 20 wt % solutions with dimensions of 12 × 5 × 0.085, 12 × 5 × 0.083, and 12 × 5 × 0.140 mm, respectively, were mounted on tension clamps. Specimens were cut from the nanowebs parallel to the production direction. The tests were run with an oscillation frequency of 1 Hz at a heating rate of 1°C/min from room temperature to 150°C. Nitrogen was used to cool the samples. The storage modulus, loss modulus, and damping factor (tan δ) data were obtained from the DMA analysis.

Contact angle measurements

A KSV Modular CAM 200 system (Yildiz Technical University, Istanbul, Turkey) was used to measure the θ's of the samples. Measurements were performed via drop shape analysis with the sessile drop technique. Experimental equipment consisted of a camera, computer, and monitor. Liquid drops were dispersed on each sample with a micrometer pipette; the image of each drop was captured by the camera connected to a computer-based image-capture system. The captured images were viewed in the monitor. The images were captured as quickly as possible after the liquid droplets were placed onto the sample surface and were photographed in less than 3 s.

RESULTS AND DISCUSSION

SEM analysis

The electrospun PET nanofiber on the collector formed a randomly oriented nonwoven web structure having nanofibers with various diameters and structures, depending on the polymer concentration.

Figure 3 shows SEM micrograph of the nanofibers electrospun from 13, 16, and 20 wt % solutions, respectively.

The shape and the size of nanofibers were governed by several parameters, including the polymer solution properties, solvent properties, and process parameters. Polymer concentration plays an important role in the spinnability and final characteristics of electrospun fibers.[20]

Generally, nanofibers with round cross sections are formed. Most fibers have a smooth surface. When the polymer concentration increases, the solution viscosity also increases in fibers with larger diameters and fewer defects.

Polyester nanofibers electrospun from the 13 wt % solution were not exactly aligned in the web. The individual fibers had a nonuniform cross section along the fiber length. Neck formation was observed in some places. The diameter of the individual fibers varied within the web with an average diameter of 0.82 μm [standard deviation (SD) = 0.312].

Polyester nanofibers electrospun from the 16 wt % solution were also not exactly aligned in the web. The individual fibers had uniform cross sections with an average diameter of 0.92 μm (SD = 0.266). Thicker fibers were obtained for the polyester nanofibers electrospun from the 20 wt % solution with uniform cross sections along the fiber length. The individual fibers had an average diameter of 3 μm (SD = 1.496).

Table I shows the diameters of the individual fibers. The average diameters of the fiber ranged from 0.82 to 3 μm, depending on polymer concentration. At lower concentrations, the electrospun fibers were still wet at the time when they reached the collector. It took a longer time to dry for the electrospun fibers. Therefore, at lower concentrations, thinner fibers were produced. In contrast, at higher concentrations, the fibers were dry by the time they reached the collector. Further elongation of the fibers was prevented. Therefore, thicker fibers were obtained. Increasing the PET concentration also led to an increase in the fiber uniformity and better alignment of the fibers in the web. However, the fiber diameter distribution within the web was broader.

The fiber thickness, fiber orientation, fiber diameter distribution, and fiber uniformity are very important structural characteristics in electrospun nanofiber webs and can alter many properties.

Viscosity measurements

Table II shows the viscosities of the different PET concentrations. An increase in the polymer concentration resulted in a higher viscosity.

Calculation of the orientation parameters for the polarized IR data

Because of the uniaxial orientation nature of the fibers arising from cylindrical symmetry, the calculation of the orientation parameters obtained from the IR data analysis was carried out with the dichroic ration (D), as defined in eq. (1):

$$D = A_{\parallel}/A_{\perp} \tag{1}$$

where $A_{\parallel}$ and $A_{\perp}$ are the measured absorbance values for the radiation polarized parallel and perpendicular to the fiber axis, respectively. To a good approximation, the dichroic ration is related to the orientation parameter [$\langle P_2(\cos\theta)\rangle$] by

$$\langle P_{200}\rangle = \langle P_2(\cos\theta)\rangle = \frac{D-1}{D+2}\frac{2}{(3\cos\alpha - 1)} \tag{2}$$

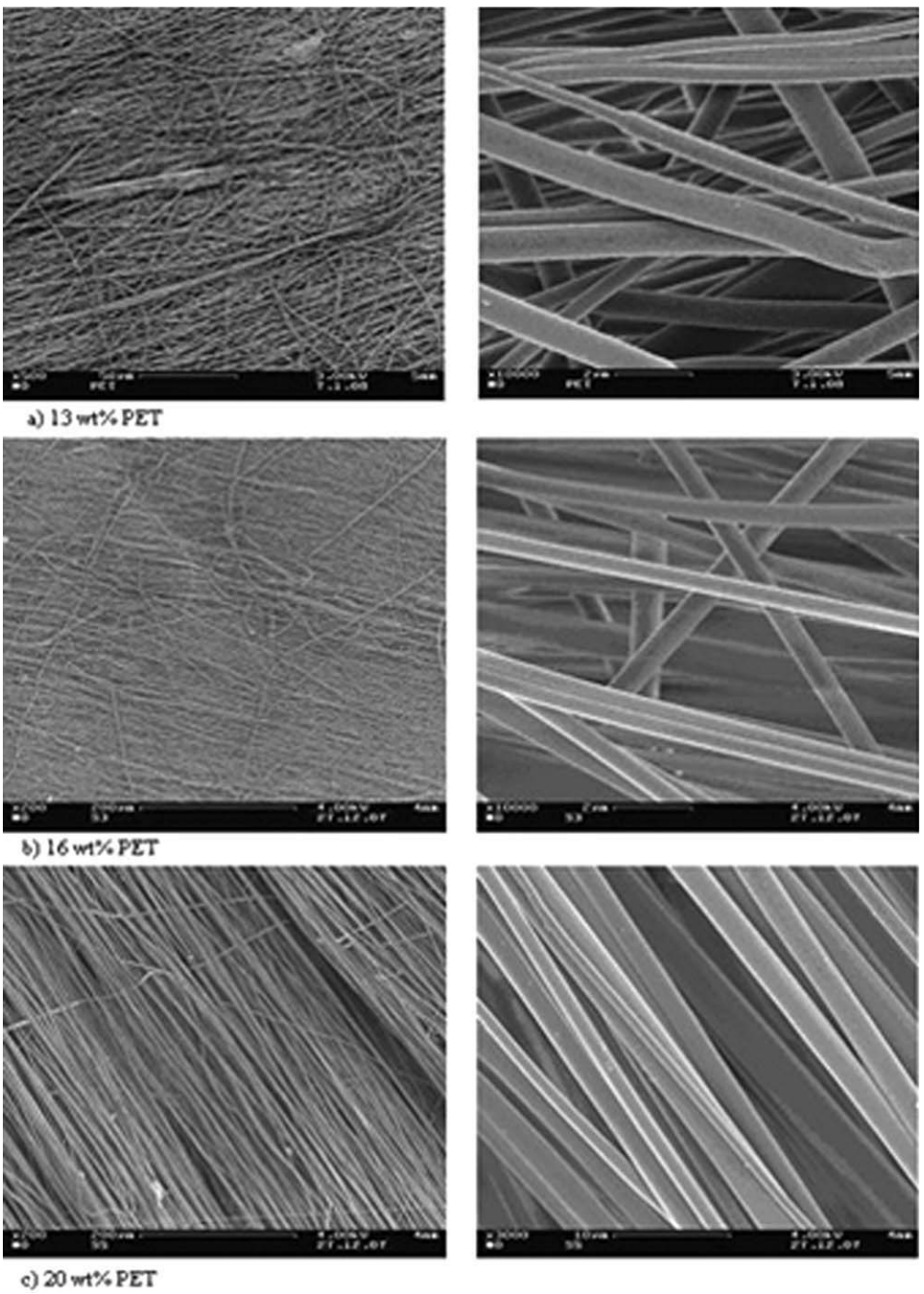

Figure 3 SEM micrographs of electrospun PET nanofibers: (a) 13, (b) 16, and (c) 20 wt % solutions.

TABLE I
Diameter Distributions of the Polyester Nanofibers with Respect to the PET Proportions

PET (wt %)	Minimum diameter (μm)	Maximum diameter (μm)	Average diameter (μm)
13	0.38	1.10	0.82
16	0.46	1.10	0.92
20	1.00	5.14	3.00

TABLE II
Viscosity Measurements of the Solutions with Respect to the PET Proportions

PET (wt %)	Viscosity (mPa s)
13	72
16	167
20	242

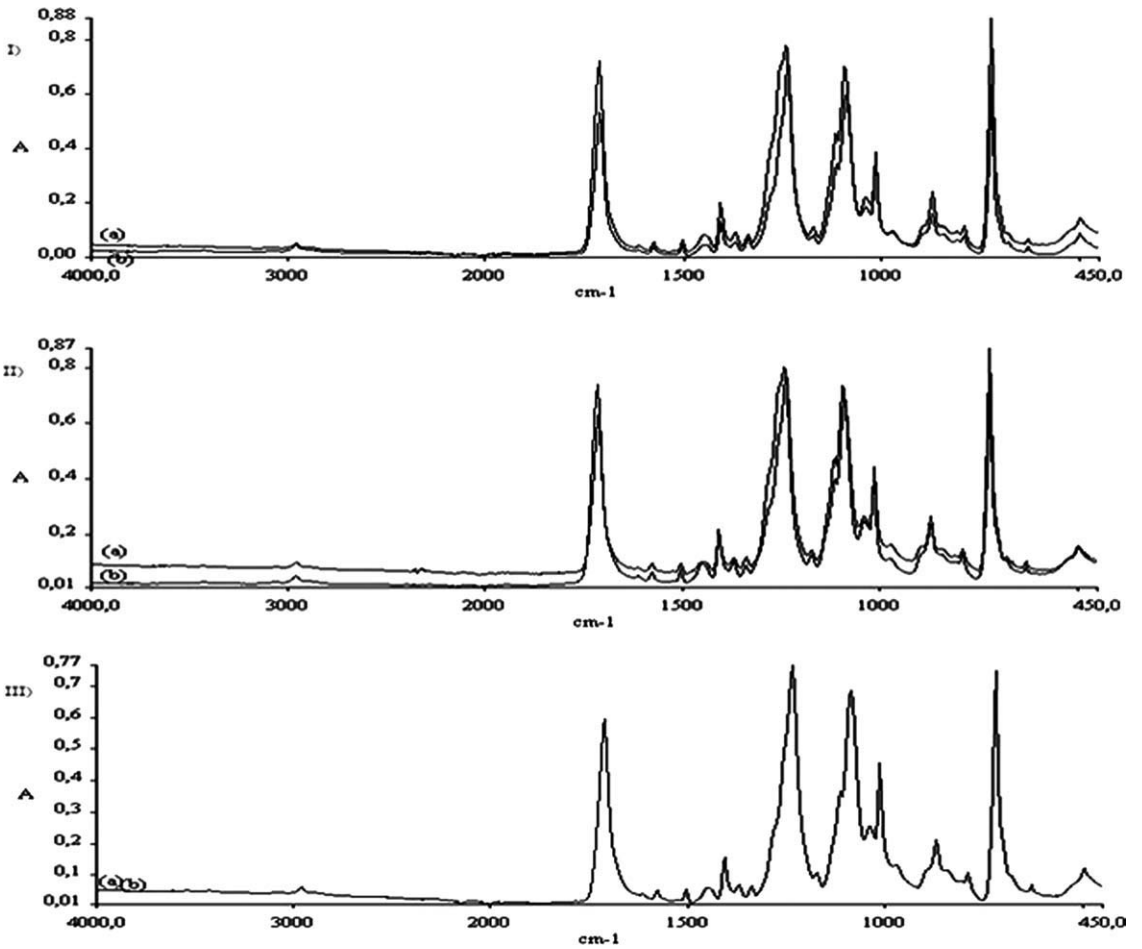

Figure 4 IR spectra of nanofibers produced from (I) 13, (II) 16, and (III) 20 wt % PET: (a) perpendicular and (b) parallel. A = absorbance.

where θ is the contact angle, or the angle between the local chain axis and the fiber axis, α is the transition moment angle between the associated vibrational mode and the chain axis, and $\langle P_{200} \rangle$ is the orientation parameter. The degree of orientation in a uniaxially aligned system can be described by the order parameter $\langle P_{200} \rangle$.[19]

In the IR spectrum of PET, the 1340- and 1370-cm^{-1} bands were assigned to the CH_2 wagging mode in the trans and gauche conformers, respectively.[21] The trans conformer is generally in crystalline regions, and the gauche conformer is in amorphous regions. Because the nanofibers produced from PET were amorphous, as seen in the wide-angle X-ray diffraction results, the 1370-cm^{-1} band was investigated for molecular orientation. The spectra of the nanofibers are shown in Figure 4. The orientation parameter ($\langle P_2 \rangle$) corresponding to the gauche conformers in the amorphous phases was evaluated with eq. (2) (see Table III). The nanofibers produced from the 13 wt % solution showed the highest molecular orientation in the amorphous regions. In the electrospinning process, the structure of the fiber was formed under the influence of two simultaneous processes, namely, the evaporation of the solvent and the elongation of the fibers. Apparently, the crystallization of the electrospun fibers were retarded because the rapid solidification of the polymer chains hindered the formation of the crystalline regions. Therefore, wide-angle X-ray diffraction results showed no crystalline structure. However, the polymer macromolecules experienced a shear force and elongational force when they flowed through the capillary, and further on within the electrospun jet, the disc collector also introduced some degree of stretching. These forces caused the polymer chains to be oriented parallel to the fiber axis in the amorphous regions. A higher polymer concentration resulted in more molecular chain entanglements

TABLE III
$\langle P_2 \rangle$ Values of the PET Nanofibers with Respect to the PET Proportions

PET (wt %)	$\langle P_2 \rangle$
13	0.18
16	0.085
20	0.024

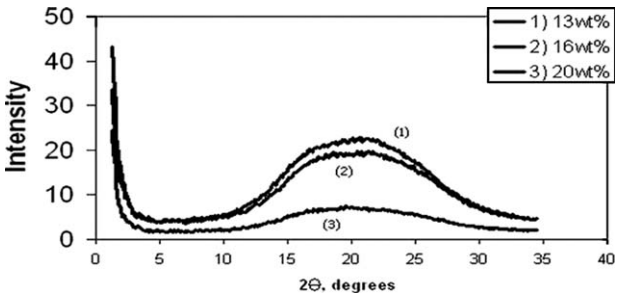

Figure 5 X-ray diffraction of the polyester nanofibers.

in the polymer solution and prevented easy molecular mobility. However, at lower concentrations, the molecules had enough freedom to align parallel to the electrospinning direction.

X-ray analysis

Figure 5 shows the X-ray diffraction pattern of the samples. There were no sharp crystalline peaks; this indicated no crystallization for the electrospun fibers. All of the curves had a broad, diffuse

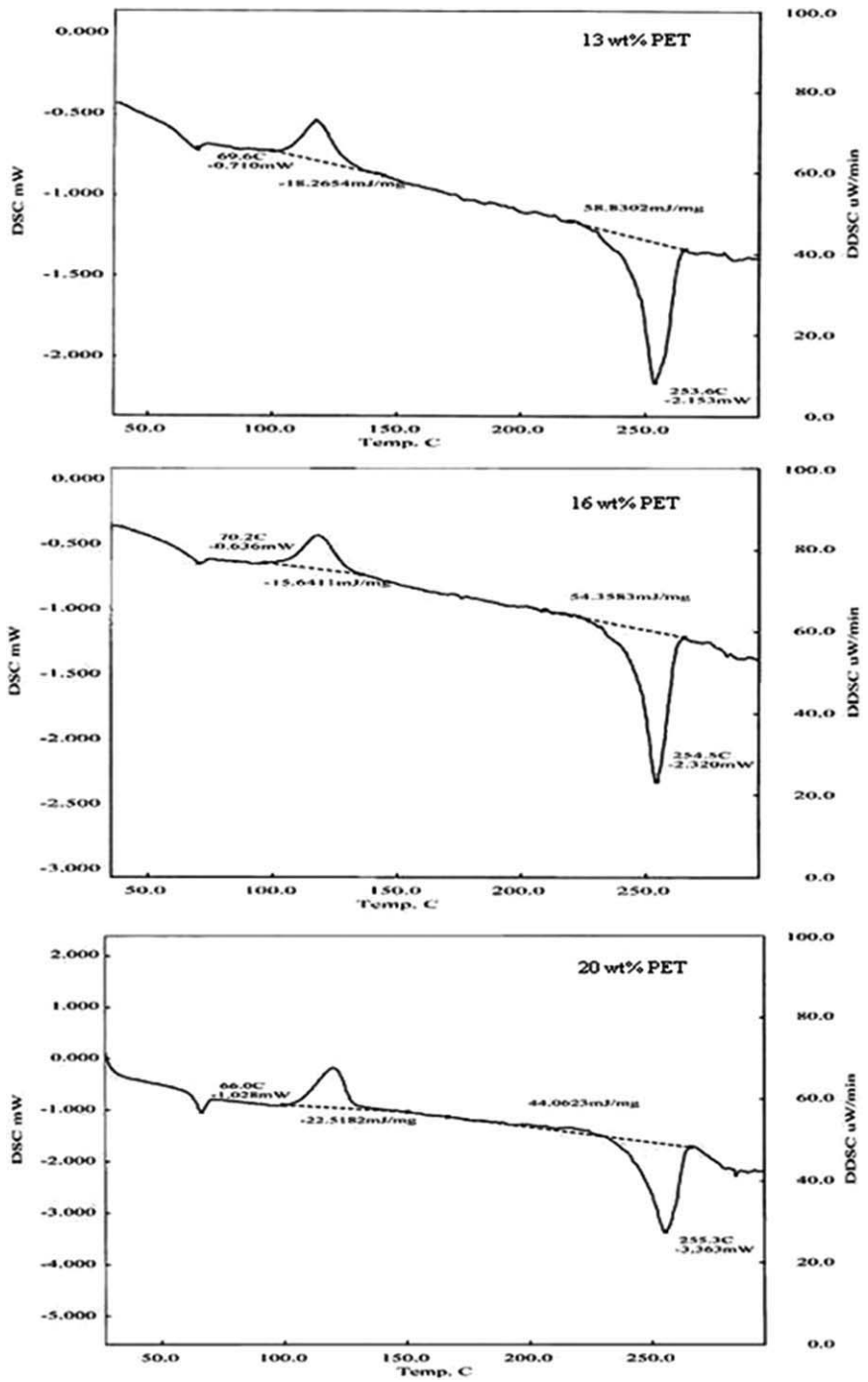

Figure 6 Differential scanning calorimetry (DSC) thermograms of the polyester nanofibers electrospun from 13, 16, and 20 wt % solutions.

TABLE IV
Data from the DSC Analysis

PET (wt %)	T_g (°C)	T_c (°C)	ΔH_c (mJ/mg)	T_m (°C)	ΔH_m (mJ/mg)
13	69.6	112.0	−18.2654	253.6	58.8302
16	70.2	114.4	−15.6411	254.5	54.3583
20	66.0	111.5	−22.5182	255.3	44.0623

T_c = crystallization temperature.

scattering profile. In the electrospinning process, crystallization of the electrospun fibers was retarded because of the rapid solidification of the polymer. The nanofibers produced from the 20 wt % solution showed weaker intensity, as it had the lowest molecular orientation in the amorphous regions.

DSC analysis

Thermal analysis of electrospun nanoweb was performed by differential scanning colorimetric analysis. Figure 6 illustrates the thermograms obtained from the electrospun nanowebs from different solutions, and Table IV shows the corresponding data. Generally, the DSC traces were typical of those expected for PET[20] and showed a very similar pattern from room temperature to 300°C. The curve had an endothermic peak around 70°C followed by a small exothermic peak around 110°C. This was further followed by a large endothermic peak around 255°C. The first endothermic peak was assigned to the glass-transition temperature (T_g) of the polymer. The second peak was the cold crystallization temperature of the polymer. Crystallizable molecular chains remained in the fiber after electrospinning and were transformed into the crystalline region during the temperature scanning of DSC. The last peak was again endothermic in nature and indicated the melting temperature (T_m). A single T_m was observed for each of the samples. This was attributed to the melting of the crystalline structure developed during the DSC scanning.

An increase in the polymer concentration also resulted in an increase in T_m and a decrease in the enthalpy of melting (ΔH_m); this indicated a decrease in the segmental mobility.

The cold crystallization peak widths for the all of the samples were almost the same; on the other hand, the cold crystallization enthalpies did not follow any pattern. Nanofibers obtained from the 20 wt % solution showed the highest crystallization enthalpy (ΔH_c); however, nanofibers electrospun from the 13 and 16 wt % solutions showed lower ΔH_c values, as they had higher molecular orientation in the amorphous regions. ΔH_c showed the amount of crystallizable free amorphous regions. A lower ΔH_c indicated a smaller amount of crystallizable free amorphous regions.

Nanofibers of the 13 and 16 wt % solutions showed higher T_g values, which indicated better molecular orientation in the amorphous structure.

TABLE V
Young's Modulus Values for the Polyester Nanowebs

PET (wt %)	Young's modulus (MPa)	Elongation at break (%)
13	2.399	41
16	3.621	35
20	2.957	–

Mechanical properties

The mechanical properties of the electrospun fibrous webs were measured by tensile tests performed in parallel with the principal axis of fiber alignment. Table V shows the Young's modulus and elongation values, and Figure 7 shows the stress–strain curves of the polyester nanofiber webs with different polymer concentrations.

The PET nanofiber web electrospun from 16 wt % solution showed the highest modulus as a result of uniform fiber diameter along the fiber length, narrow diameter distribution in the web, and their higher molecular orientation. Nanofiber webs electrospun from the 13 and 16 wt % solutions had similar elongations at break; on the other hand, the nanofiber web electrospun from 20 wt % solution was highly ductile, and the material elongated without break, as it had the worst molecular orientation in the amorphous regions.

The stress–strain curves of the nanofiber webs prepared from the 13 and 16 wt % solutions were similar. An initial linear portion of the stress–strain

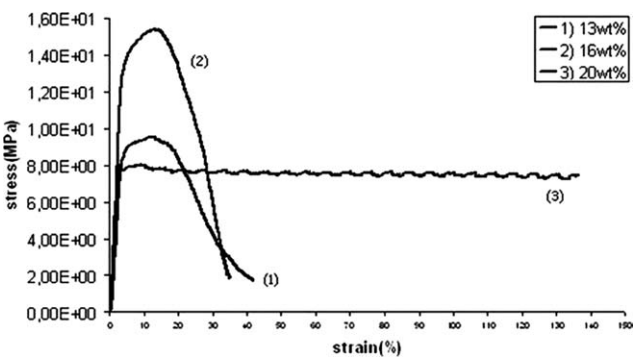

Figure 7 Stress–strain curves of the polyester nanowebs.

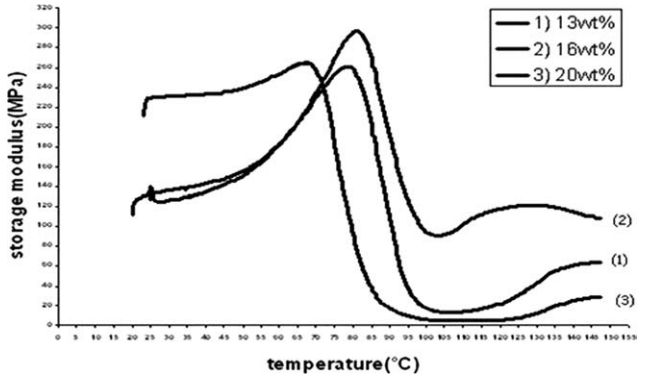

Figure 8 Storage modulus versus temperature curves of the polyester nanofiber webs.

curve was observed for all of the nanofiber webs. The initial part of the stress–strain curve exhibited the typical elastic behavior and was affected by the nanofiber web characteristics, such as fiber orientation, fiber uniformity, and fiber diameter distribution. The initial part of the curve also determined Young's modulus and showed the resistance to plastic deformation. Individual fiber properties, such as fiber diameter and fine structure, showed no important effect in the initial part of the curve. After a linear initial part, a yield region was observed. A clear reduction in the web width was observed as a result of the reorientation and slippage of the fibers. The yield region was followed by a gradual reduction in the stress–strain dependence due to fiber breakages. The last part of the stress–strain curve was more affected by the individual fiber properties. The stress–strain curve of the nanoweb electrospun from the 20 wt % solution showed a yield point rather than a region, and the material elongated without breaking.

However, the properties of the individual fibers played an important role in the overall mechanical performance of the nanoweb.

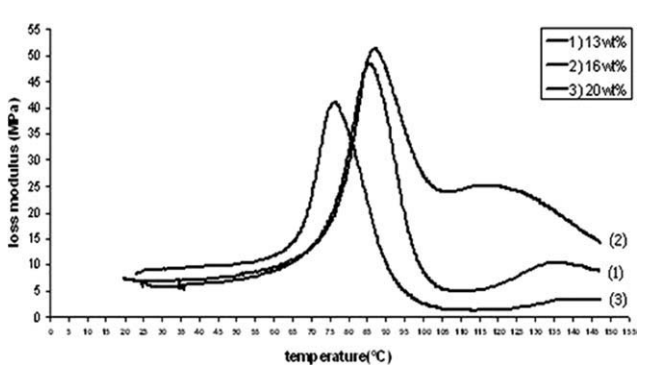

Figure 9 Loss modulus versus temperature curves of the polyester nanofiber webs.

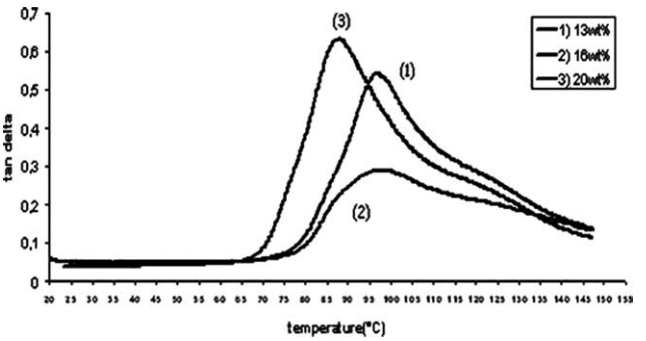

Figure 10 Tan δ versus temperature curves of the polyester nanofiber webs.

DMA tests

Dynamic mechanical properties are the mechanical properties of materials as they are deformed under periodic forces. The dynamic modulus, loss modulus, and mechanical damping (tan δ) explain these properties.

The dynamic modulus is approximately similar to the Young's or elastic modulus, or stiffness. The dynamic loss modulus is a measure of the energy absorbed due to relaxation and is useful in understanding the mechanisms of internal motions. Generally, in thermoplastics, the storage and loss moduli change with temperature as the molecular mobility is affected.

The tan δ is the ratio of the loss modulus to the dynamic modulus and is used to determine the glass-transition region. The dynamic mechanical properties of polymers are usually studied over a wide temperature range.[22]

Figures 8–10 show the storage modulus, loss modulus, and tan δ values, respectively, of the electrospun nanowebs. Table VI gives the T_g and Young's modulus values. The tan δ curves of the nanowebs obtained from DMA analysis showed similar behavior. The observed peaks were not symmetrical with a broadening to higher temperatures. This suggested a variety of chain conformations at higher temperatures. The peak was caused by the glass-transition behavior. The tan δ curve of the nanoweb electrospun from the 16 wt % solution had a smaller but broader peak at higher temperature. This was inferred to be caused by a relatively higher content

TABLE VI
Young's Modulus and T_g Values for the Polyester Nanowebs

PET (wt %)	Young's modulus (MPa)	T_g (°C)
13	124	96
16	127	98
20	229	87

of extended molecular chain in the amorphous structure.[23] This was also confirmed by the ATR FTIR analysis. This increase in the noncrystalline orientation played an important role in improving the mechanical behavior.

Figures 8 and 9 show the storage modulus and loss modulus of the samples. As expected, the nanoweb electrospun from the 20 wt % solution showed the highest storage modulus at lower temperatures. However, at higher temperatures near T_g, the PET nanoweb electrospun from the 16 wt % solution showed a higher storage modulus, whereas the others were approximately the same.

The nanoweb produced from the 20 wt % solution showed a plateau region at the lower temperature followed by a slight increase before a rapid drop starting from about 70°C; this was due to the onset of relaxation processes in the disordered region. However, the samples produced from the 16 and 13 wt % solutions were similar in their relative values and shapes. The nanoweb produced from the 16 wt % solution showed a slight increase in the modulus at about 130°C. This was attributed to the crystallization phenomenon during the heating process, as it had a better molecular orientation in the disordered regions.

Contact angle measurements

It is well known that atoms at a free surface experience a different local environment than do atoms in the bulk of a material; as a result, the energy associated with these atoms will, in general, be different from that of the atoms in the bulk. The excess energy associated with surface atoms is called *surface free energy* (γ). In traditional continuum mechanics, such γ is typically neglected because it is associated with only a few layers of atoms near the surface, and the ratio of the volume occupied by the surface atoms to the total volume of material of interest is extremely small. However, when the fiber diameter decreases, the surface-to-volume ratio becomes significant and so does the effect of the γ. Because of the drastic reduction in the fiber diameter for nanofibers, most of the molecules in the fiber lay on the or near the surface. The surface energy of the fibers is one of the main characteristics because it determines the potential level of interactions that the fibers are able to have with other fibers. It is necessary to know the surface energy to understand many surface characteristics, such as wettability, adhesion, friction, and absorption.[24] Schonhorn and Ryan[25] showed that surface tension of polyethylene crystals depended on the crystallinity of the surface. They found that the surface tension values increased with increasing crystallinity of the surface. As nanofibers produced from the 13 wt % solution had the highest molecular orientation in the amorphous regions, they showed the highest surface energy.

TABLE VII
θ and γ Values for the Polyester Nanofibers

PET (wt %)	θ (°)	γ (mN/m)
13	104.23	204.17
16	130.27	78.90
20	160.42	70.16

Table VII shows the θ and γ values for the electrospun PET nanofibers with different polymer concentrations.

An increase in the polymer concentration increased θ of the nanoweb surfaces; however, it lowered the γ values. The PET fibers exhibited a θ around 70–75°C, which was associated with low γ. A reduction in the fiber diameter of PET resulted in a superhydrophobic surface.[24]

CONCLUSIONS

Electrospinning was successfully used to produce PET nanofibrous webs with TFA and DCM mixture as a solvent. The effects of the polymer concentration on the mechanical, thermal, and surface properties under the same electrospinning conditions were investigated. Increasing PET concentration led to an increase in the fiber uniformity, better alignment of the fibers in the web, and thicker fibers. However, the fiber diameter distribution in the web was broader. The PET nanofiber web electrospun from the 16 wt % solution showed the highest modulus as a result of the uniform fiber diameter along the fiber length, the narrow diameter distribution in the web, and the higher molecular orientation. Nanofiber webs electrospun from the 13 and 16 wt % solutions had similar elongations at break; on the other hand, the nanofiber web electrospun from the 20 wt % solution was highly ductile, and the material elongated without break because it had the lowest molecular orientation in the amorphous regions.

X-ray results showed that because of the rapid solidification of the fibers, crystallization was retarded. ATR FTIR results gave information about the molecular orientation in the amorphous regions. A higher polymer concentration resulted in more molecular chain entanglements in the polymer solution and prevented easy molecular mobility. However, at lower concentrations, the molecules had enough freedom to align in the electrospinning direction. The nanofibers produced from the 13 wt % solution showed the best molecular orientation in the amorphous regions. DSC results indicated that nanoweb of the 13 and 16 wt % solutions had higher T_g's; this indicated better molecular orientation in the amorphous structure.

The tan δ curve of the nanoweb electrospun from the 16 wt % solution had a smaller but broader peak at higher temperatures. This was attributed to the relatively higher content of extended molecular chains in the amorphous structure. This increase in noncrystalline orientation played an important role in improving the mechanical behavior.

θ measurements showed very high θ values for the samples; this indicated that the PET nanofiber webs had superhydrophobic surface characteristics.

The results show that nanoweb of the 16 wt % solution had better mechanical and thermal behavior because of the increased molecular orientation in the amorphous structure and narrower fiber diameter distribution in the web.

References

1. Reneker, D. H.; Yarin, A. L.; Zussman, E.; Xu, H. Adv Appl Mech 2007, 41, 43.
2. Zussman, E.; Theron, A.; Yarin, A. L. Appl Phys Lett 2003, 82, 973.
3. Greiner, A.; Wendorff, J. H. Angew Chem 2007, 46, 5670.
4. Frenot, A.; Chronakis, I. S. Curr Opin Colloid Interface Sci 2003, 8, 64.
5. Subbiah, T.; Bhat, G. S.; Tock, R. W.; Parameswaran, S.; Ramkumar, S. S. J Appl Polym Sci 2005, 96, 557.
6. Zussman, E.; Burman, M.; Yarin, A. L.; Khalfin, R.; Cohen, Y. J Polym Sci Part B: Polym Phys 2006, 44, 1482.
7. Arinstein, A.; Burman, M.; Gendelman, O.; Zussman, E. Nat Nanotechnol 2007, 2, 59.
8. Reneker, D. H.; Yarin, A. L.; Fong, H.; Koombhongse, S. J Appl Phys 2000, 87, 4531.
9. Theron, A.; Zussman, E.; Yarin, A. L. Nanotechnol J 2001, 12, 384.
10. Theron, A.; Zussman, E.; Yarin, A. L. Polymer 2004, 45, 2017.
11. Lee, K. H.; Kim, H. Y.; Khil, M. S.; Ra, Y. M.; Lee, D. R. Polymer 2003, 44, 287.
12. Mo, X. M.; Xu, C. Y.; Kotaki, M.; Ramakrishna, S. Biomaterials 2004, 25, 1883.
13. Kim, K. W.; Lee, K. H.; Khil, M. S.; Ho, Y. S.; Kim, H. Y. Fibers Polym 2004, 5, 122.
14. Veleirinho, B.; Lopes-da-Silva, J. A. Process Biochem 2004, 44, 353.
15. Hong, K. H.; Kang, T. J. J Appl Polym Sci 2006, 100, 167.
16. Jung, K. H.; Huh, M. W.; Meng, W.; Yuan, J.; Hyun, S. H.; Bae, J. S.; Hudson, S. M.; Kang, I. K. J Appl Polym Sci 2007, 105, 2816.
17. Ma, Z.; Kotaki, M.; Young, T.; He, W.; Ramakrishna, S. Biomaterials 2005, 26, 2527.
18. Lopes-da-Silva, J. A.; Veleirinho, B.; Delgadillo, I. J Nanosci Nanotechnol 2009, 9, 3798.
19. Karacan, I. J Appl Polym Sci 2006, 100, 142.
20. Velerinho, B.; Rei, M. F.; Lopes-da-Silva, J. A. J Polym Sci Part B: Polym Phys 2007, 46, 460.
21. Zhang, W.; Shen, D. Polym J 1998, 30, 4, 311.
22. Yang, S.; Taha-Tijerina, J.; Serrato-Diaz, V.; Hernandez, K.; Lozano, K. Compos B 2007, 38, 228.
23. Wu, G.; Jiang, J.; Tucker, P. A.; Cuculo, J. A. J Polym Sci Part B: Polym Phys 1996, 34, 2035.
24. Hsieh, Y. In Surface Characteristics of Fibers and Textiles; Pastore, C. M.; Kiekens, P., Eds.; Marcel Dekker: New York, 2001; p 33.
25. Schonhorn, H.; Ryan, F. W. J Phys Chem 1966, 70, 3811.